Electronic Supplementary Material (ESI) for Nanoscale.

# Supporting Information

# $SnS_2/TiO_2$ Nanohybrids Chemically Bonded on Nitrogen-doped Graphene for Lithium-Sulfur Batteries: Synergy of Vacancy Defects and Heterostructure

Xuecheng Li [a], Guanlun Guo [b], Ning Qin [c], Zhao Deng [a], Zhouguang Lu [c], Dong Shen [d], Xu Zhao [e], Yu Li [a], Bao-Lian Su [a,f], Hong-En Wang [a,*]

[a] State Key Laboratory of Advanced Technology for Materials Synthesis and Processing, Wuhan University of Technology, Wuhan, 430070, China. Email: hongenwang@whut.edu.cn

[b] Hubei Key Laboratory of Advanced Technology for Automotive Components & Hubei Collaborative Innovation Center for Automotive Components Technology, Wuhan University of Technology, Wuhan 430070, China.

[c] Department of Materials Science and Engineering, Southern University of Science and Technology of China, Shenzhen, China.

[d] Department of Chemistry and Center Of Super-Diamond and Advanced Films (COSDAF), City University of Hong Kong, HKSAR, China.

[e] Department of Materials Science and Engineering, Harbin Institute of Technology, Harbin, 150001, China.

[f] Laboratory of Inorganic Materials Chemistry (CMI), University of Namur, 61 rue de Bruxelles, B-5000 Namur, Belgium.

## Experimental

### Materials synthesis.

### *Synthesis of N-doped graphene (NG) nanosheets.*

First, 60 mg graphene oxide (GO) powders were dispersed in 60 mL deionized water and sonicated for 3 h, then 0.3 mL poly (diallyldimethylammonium chloride) (PDDA) solution (20 wt%) was added and further ultrasonicated for 1 h to form a uniform surface-modified suspension. Next, 0.7 g thioacetamide (TAA) was added into the suspension and stirred for 30 min. Then, 100 μL ethylenediamine (EDA) solution was added and further stirred for 15 min. The resulting mixture was transferred to 100 mL Teflon-lined autoclave, sealed and heated at 180 °C for 20 h. The final precipitates were harvested by centrifugation, washed with deionized water, and freeze-dried for 48 h to obtain the N-doped reduced graphene oxide (denoted as "NG").

### *Synthesis of NG/$SnS_2$ nanocomposites.*

Firstly, 60 mg graphene oxide (GO) powders were dispersed in 60 mL deionized water and ultrasonicated for 3 h, then 0.3 mL PDDA solution (20 wt%) was added and further sonicated for another 1 h to fully disperse the GO powders and functionalize their surface to be negatively charged. Next, 0.7 g $SnCl_4 \cdot 5H_2O$ and 0.7 g thioacetamide (TAA) were successively dissolved in the GO aqueous solution at room temperature by vigorously stirring for 30 min, and finally 100 μL EDA was added into the mixture under magnetic stirring. The resulting mixture was transferred to 100 mL Teflon-lined autoclave, sealed and heated at 180 °C for 20 h. During this process, the $Sn^{4+}$ ions were adsorbed on GO surface and then reacted with $S^{2-}$ released from decomposition of TAA to form $SnS_2$ nanosheets. Meanwhile, EDA was used to *in situ* reduce

GO and dope nitrogen into graphene during hydrothermal process. The final precipitates were harvested by centrifugation, washed with deionized water and freeze-dried for 48 h to obtain the N-doped graphene/$SnS_2$ (denoted as NG/$SnS_2$) nanocomposites.

***Synthesis of NG/$SnS_2$/$TiO_2$ nanocomposites.***

The NG/$SnS_2$ nanocomposites were dispersed into 80 mL acetone containing 0.5 mL deionized water by ultrasonication for 30 min. Meantime, 0.5 mL tetrabutyl titanate (TBT) was dissolved into 20 mL ethylene glycol by vigorously stirring for 30 minutes to form titanium glycolates (TEG) sol. Then, the sol was dropwise added into the acetone bath containing NG/$SnS_2$ under vigorous stirring for 1 h. The resulting precipitates were filtered and washed with deionized water and then re-dispersed into deionized water (100 mL), followed by heating at 95 °C for 12 h to convert the TEG into $TiO_2$ nanocrystals. Finally, the NG/$SnS_2$/$TiO_2$ nanocomposites were collected by centrifugation and washed with ethanol and deionized water in sequence, and finally freeze-dried.

**Materials characterizations.**

X-ray diffraction (XRD) patterns were recorded on a Bruker diffractometer with Cu Kα radiation ($\lambda$=0.154056 nm) at 40 kV/mA. The morphologies of the samples were observed using scanning electron microscope (SEM, Hitachi S-4800) equipped with an energy-dispersive X-ray (EDX) spectroscope. Transmission electron microscopy (TEM) and high-solution TEM (HRTEM) micrographs were acquired on a JEOL JEM-2100F microscope with an acceleration voltage of 200 kV. The surface elemental composition and electronic states were analyzed by an X-ray photoelectron spectroscope (XPD, Thermo fisher, Alpha). The binding energies (BE) for the samples were calibrated using C 1s peak from a carbon tape at 284.8 eV. Thermogravimetry analyses (TGA) were recorded using a SETARAM Labsys Evo S60/58458 thermal analyzer under a flow of air (or Ar) with a heating rate of 5 °C $min^{-1}$. The Brunner–Emmett–Teller (BET) specific surface area and Barrett–Joyner–Halenda (BJH) pore size distribution were determined through $N_2$ adsorption/desorption isotherms at 77 K on a Tri Star II 3020 surface area and porosity analyzer. Prior to sorption experiments, the samples were degassed at 100 °C for 48 h under vacuum. Raman measurements were recorded on a Nexus FTIR spectrometer using a 1064 nm laser. Electron paramagnetic resonance (EPR) signals were measured using a Bruker EMX plus-10/12 with a Microwave Bridge (microwave frequency, 9.853 GHz; microwave power, 20 mW; modulation amplitude, 4 G; modulation frequency, 100 kHz) at room temperature.

**Polysulfide adsorption tests.**

The $Li_2S_4$ solution (20 mM) were prepared by dissolving the sulfur and $Li_2S$ with a stoichiometric molar ratio of 3:1 in DOL/DME (1:1, v/v) in an Ar-filled glovebox. The solution was stirred for 24 h at 50 °C to form a 20 mM $Li_2S_4$ stock solution. Then, 25 mg active materials (NG/$SnS_2$ or NG/$SnS_2$/$TiO_2$) was separately added into 3 mL of the above $Li_2S_4$ solution for adsorption test.

**Electrochemical measurements.**

***Electrochemical tests*.**

The electrochemical tests were performed by using CR2025 coin-type cells, lithium foils as the counter/reference electrode and microporous membrane (Celgard 2400) as the separator. The working electrodes were prepared by blending active material, acetylene black, and polyvinylidene fluoride (PVDF) binder with a weight ratio of 8:1:1 in N-methyl-2-pyrrolidone (NMP) to form a slurry. The slurry was uniformly coated on Al foils and dried at 55 $^{o}$C for 12 h under vacuum and then cut into circular disks with an average active material loading of ~1.2 mg cm$^{-2}$. The electrolyte was 1.0 M solution of lithium bis(trifluoromethanesulfonyl)imide (LiTFSI) with 1 wt% $LiNO_3$ dissolved in 1,3-dioxolane (DOL) and 1,2-dimethoxy ethane (DME) (1:1, v/v) and the ratio of electrolyte : sulfur was fixed at about 10 mL g$^{-1}$. The coin cells were assembled in an ultrapure argon-filled glovebox with both the moisture and the oxygen content below 0.3 ppm. Galvanostatic charge/discharge tests were conducted using a LAND-CT2001A within a potential window of 1.4~2.8 V vs. $Li^+/Li$ at different current densities. Cyclic voltammetry (CV) curves were recorded an electrochemical workstation (CHI 604e) within a potential window of 1.4~2.8 V at a scan rate of 0.2 mV s$^{-1}$. Electrochemical impedance spectroscopy (EIS) was performed on an electrochemical workstation (Autolab PGSTAT 302N) at the frequency region of 100 kHz to 10 mHz.

***Symmetrical cell assembly and CV measurements.***

The electrodes used for symmetrical cells were assembled using active materials ($NG/SnS_2$ or $NG/SnS_2/TiO_2$). First, 0.2 M $Li_2S_6$ solution was prepared by dissolving sulfur powder and $Li_2S$ with a molar ratio of 5:1 in DOL/DME (1:1, v/v) and used as electrolyte for symmetrical cells. Then, the active materials and PVDF binder with a mass ratio of 4:1 were dispersed in NMP to form a uniform slurry. The resultant slurry was coated on Al foils and dried for 12 h at 120 $^{o}$C under vacuum and then cut into circular disks as both working and counter electrodes. CV measurements of the symmetrical cells were performed at different scan rates to probe the conversion kinetics of polysulfides on the electrode surface.

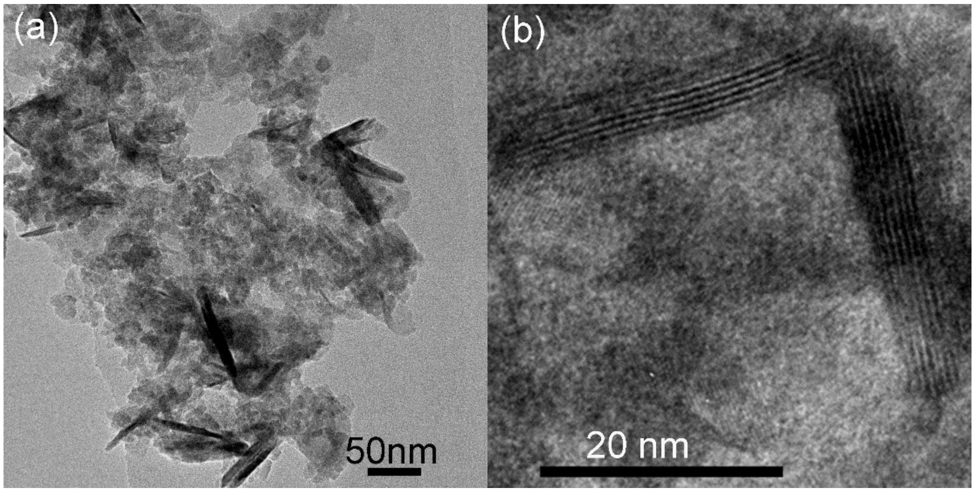

Figure S1. (a) low- and (b) high-magnification TEM images of NG/$SnS_2$/$TiO_2$ product, showing that most of the $SnS_2$ nanosheets have been vertically grown on the N-doped graphene.

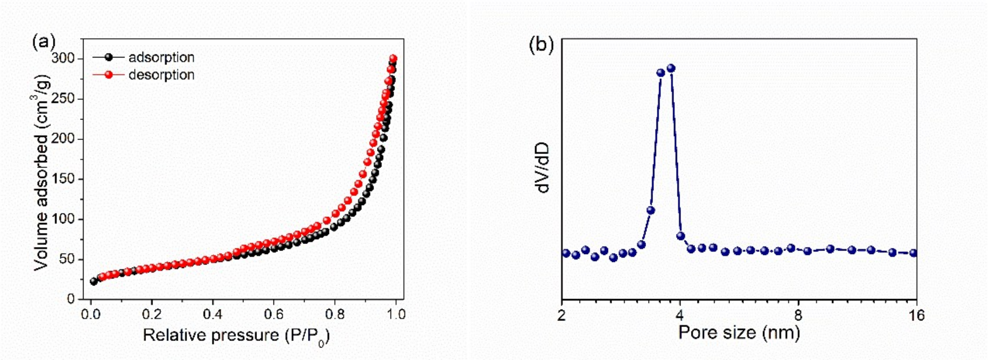

Figure S2. Nitrogen adsorption-desorption isotherm (a) and pore size distribution plot (b) of the as-prepared NG/$SnS_2$/$TiO_2$ sample.

Nitrogen adsorption/desorption experiments were performed to study the pore structure of the NG/$SnS_2$/$TiO_2$ sample. The isotherms (Figure S2a) shows a type-IV curve with a type-III hysteresis loop characteristic of mesoporous materials with slit-shape pores formed by the cross-linking of lamellar nanosheets. The BET specific surface area and pore volume are estimated to be *ca.* 137 $m^2$ $g^{-1}$ and ~0.5 $cm^3$ $g^{-1}$, respectively. BJH pore size distribution analysis yields a relatively narrow pore diameter distribution centering around ~4 nm (Figure S2b).

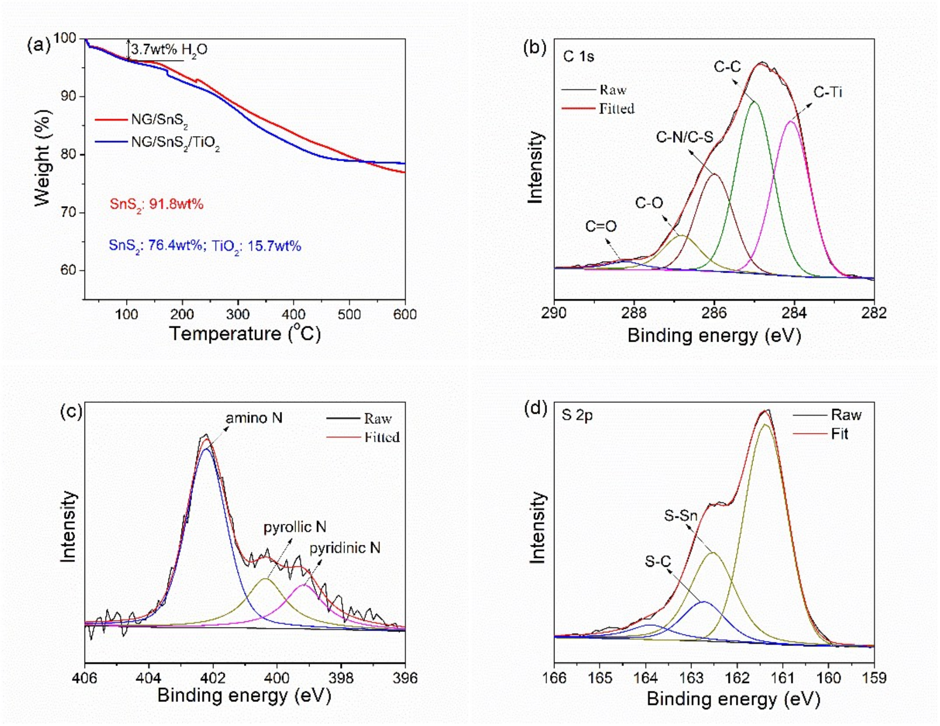

Figure S3. (a) Thermogravimetric (TG) curves of NG/$SnS_2$ and NG/$SnS_2$/$TiO_2$ products in air with a temperature ramping rate of 5 °C/min. XPS spectra of (b) C 1s, (c) N 1s and (d) S 2p core levels in NG/$SnS_2$/$TiO_2$ sample.

After heating in Air, $SnS_2$ would be oxidized to $SnO_2$ and graphene can be thoroughly decomposed. The weight fraction of $SnS_2$ content in the NG/$SnS_2$ product is 91.8%; whereas the mass contents of $SnS_2$ and $TiO_2$ in the NG/$SnS_2$/$TiO_2$ sample are 76.4% and 15.7%, respectively (Figure S3a).

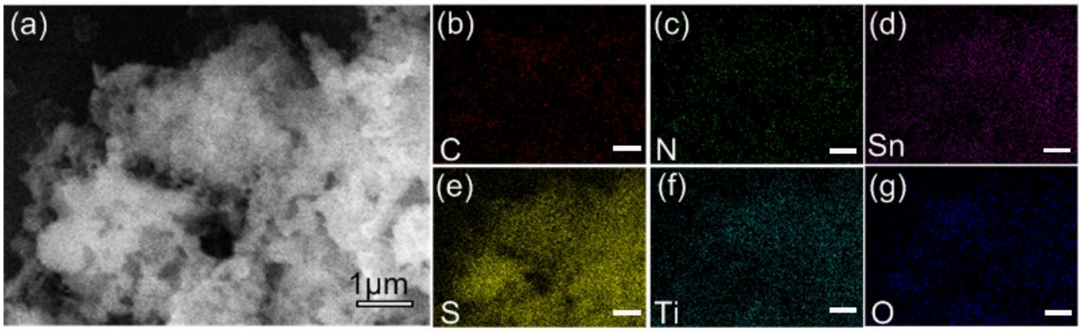

Figure S4. SEM (a) and elemental mapping images of (h) C, (i) N, (j) Sn, (k) S, (l) Ti, (m) O in $NG/SnS_2/TiO_2$-S cathode. Scale bars of (b-g) are all 1 μm.

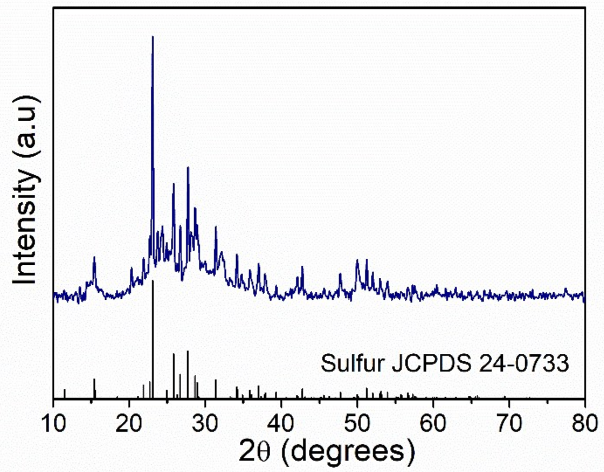

Figure S5. XRD pattern of NG/$SnS_2$/$TiO_2$-S.

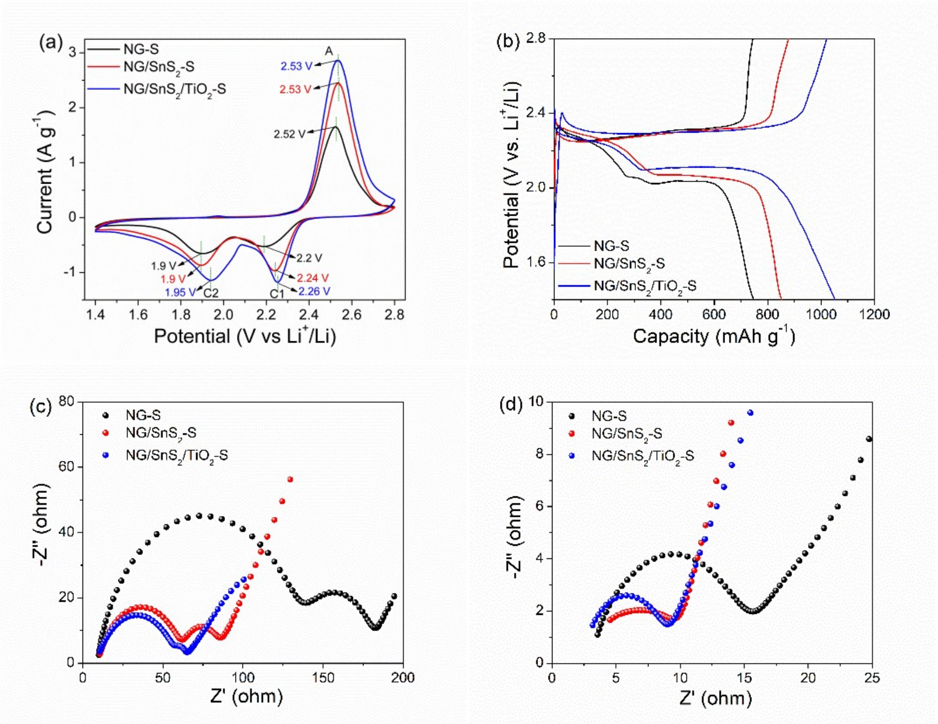

Figure S6. Cyclic voltammetry (CV) curves (a) and the 3rd galvanostatic charge/discharge curves (b) of NG-S, NG/SnS$_2$-S and NG/SnS$_2$/TiO$_2$-S electrodes at 0.2 C; electrochemical impedance spectra (EIS) of NG-S, NG/SnS$_2$-S and NG/SnS$_2$/TiO$_2$-S electrode in fresh cells (c) and after 500 cycles at 0.5 C (d), respectively.

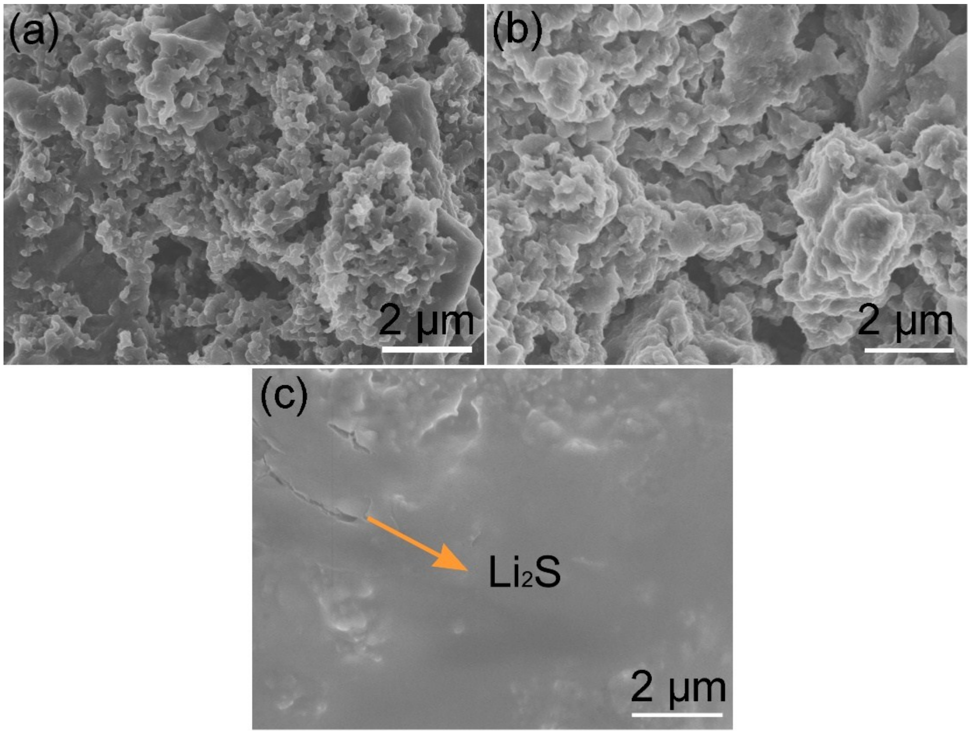

Figure S7. SEM images of (a) NG/$SnS_2$-S and (b) NG/$SnS_2$/$TiO_2$-S electrodes after discharge to 1.4 V over 500 cycles at 0.5 C.

Table S1. A comparison of the electrochemical performance between this work and some other Li-S batteries.

| Cathode | Current density (C) | Cycle number | Capacity retention ratio (%) | Reference |
|---|---|---|---|---|
| **This work** | **0.5** | **500** | **68** | |
| S/C-$SnS_2$-10 | 0.5 | 300 | 60.1 | [1] |
| TiO@C-HS/S | 0.5 | 500 | 59.1 | [2] |
| S/$NiS_2$-C | 2 | 500 | 54.9 | [3] |
| $MoS_2$ | 0.2 | 50 | 63.2 | [4] |
| G/S | 0.5 | 100 | 49.9 | [5] |
| G-$VS_2$/S | 0.5 | 100 | 67.1 | [5] |
| $MoS_{2-X}$/rGO/S | 0.5 | 600 | 54.2 | [6] |
| $MoS_2$/rGO/S | 0.5 | 150 | 55.8 | [6] |
| Fe-PGM-S | 2 | 500 | 54 | [7] |

**References:**

[1] M. Li, J.B. Zhou, J. Zhou, C. Guo, Y. Han, Y.C. Zhu, G.M. Wang, Y.T. Qian, Mater. Res. Bull. 96 (2017) 509–515.

[2] Z. Li, J.T. Zhang, B.Y. Guan, D. Wang, L.M. Liu, X.W. Lou, Nat. Commun. 7 (2016) 13065.

[3] Y. Lu, X. Li, J. Liang, L. Hu, Y. Zhu, Y. Qian, Nanoscale 8 (2016) 17616.

[4] D.-A. Zhang, Q. Wang, Q. Wang, J. Sun, L.-L. Xing, X.-Y. Xue, Electrochim. Acta, 173 (2015) 476.

[5] X.Y. Zhu, W. Zhao, Y.Z. Song, Q.C. Li, F. Ding, J.Y. Sun, L. Zhang, Z.F. Liu, Adv. Energy Mater. (2018) 1800201.

[6] H.B. Lin, L.Q. Yang, X. Jiang, G.C. Li, T.R. Zhang, Q.F. Yao, G. W. Zheng, J.Y. Lee, Energy Environ. Sci. 10 (2017) 1476.

[7] C. Zheng, S.Z. Niu, W. Lv, G.M. Zhou, J. Li, S.X. Fan, Y.Q. Deng, Z.Z. Pan, B.H. Li, F.Y. Kang, Q.H. Yang, Nano Energy, 33 (2017) 306–312.